



ELSEVIER

Contents lists available at ScienceDirect

Chinese Chemical Letters

journal homepage: www.elsevier.com/locate/cclet

Communication

Electropolymerization of cobalt porphyrins and corroles for the oxygen evolution reaction

Qingxin Zhang, Yabo Wang, Yanzhi Wang, Shujiao Yang, Xuan Wu, Bin Lv, Ni Wang, Yimei Gao, Xiaoran Xu, Haitao Lei*, Rui Cao*

Key Laboratory of Applied Surface and Colloid Chemistry, Ministry of Education, School of Chemistry and Chemical Engineering, Shaanxi Normal University, Xi'an 710119, China

ARTICLE INFO

Article history:

Received 16 March 2021

Revised 22 April 2021

Accepted 25 April 2021

Available online xxx

Keywords:

Cobalt corroles

Cobalt porphyrins

Electropolymerization

Molecular electrocatalysis

Oxygen evolution

ABSTRACT

Developing large-scale electrocatalysts using molecular complexes for the oxygen evolution reaction (OER) is of great importance. Herein, four cobalt porphyrins and corroles are deposited on electrode substrates using a simple and fast electropolymerization method. Our results showed that **Co-1-P@CC**, formed by electropolymerizing Co tetrakis(*p*-N-pyrrolylphenyl)porphyrin (**Co-1-P**) on carbon cloth (CC), is the most active OER catalyst in the examined Co porphyrins and corroles in alkaline aqueous solutions by displaying an onset overpotential of 380 mV. Long-term electrolysis tests confirmed the stability of these electropolymerized films by functioning as OER electrocatalysts.

© 2021 Published by Elsevier B.V. on behalf of Chinese Chemical Society and Institute of Materia Medica, Chinese Academy of Medical Sciences.

The increasing threat of the intense global energy demands and pressing environmental concerns have activated extensive research on clean energy conversion and storage systems with high efficiency, low-cost and environmental benignity [1–6]. Hydrogen is considered to be one of the most ideal energy sources due to its good combustion performance, ideal heating value, and wide utilization forms [7,8]. Water splitting is regarded as one of the most effective methods to generate H₂ [1,9–14].

Water splitting involves two half reactions: hydrogen evolution reaction (HER) and oxygen evolution reaction (OER). OER, as one of the half reactions of water splitting, is challenging both thermodynamically (2H₂O → O₂ + 4H⁺ + 4e⁻, ΔE = 1.23 V vs. normal hydrogen electrode) and kinetically (significant rearrangement of atoms) [13]. Therefore, the design and development of highly active and stable catalysts for OER is urgently needed for energy conversion. As a result, chemists and material scientists have paid tremendous efforts in this area. In the past decades, RuO₂ and IrO₂ are considered to be the best OER catalysts in both acidic and alkaline environments [15–19]. Despite their high activity, the large scale use of these noble-metal-based catalysts is limited by their low natural abundance and high cost [20]. As an alternative strategy, cheap first-row transition-metal-based materials and

complexes have been largely studied as electrocatalysts for OER [21–31].

For many decades, porphyrin derivatives have attracted great interests and have been widely studied in many research areas due to their unique structures and properties [21,22,32–37]. Metal porphyrins and corroles are also a class of promising electrocatalysts because of their robust property in both acidic and basic solutions. However, most molecular catalysts are used in homogeneous catalysis, which not only has low utilizations but also has great limitations in practical applications. There are two main reasons: one is that only a small fraction of the catalyst in the diffusion layer will work in the catalytic process; the other is that products separation and catalyst regeneration are difficult. To address these issues, several strategies have been developed to make molecular catalysts heterogeneous. An efficient approach is covalent or noncovalent grafting of molecular catalysts on conductive materials, such as graphenes, carbon nanotubes, metal oxides [38–50]. Although considerable efforts have been devoted to grafting molecular catalysts on conductive materials, there is still a problem that the amount of loaded catalysts may be too small. Electrodeposition is widely used to produce metal-based material catalysts, which has proven to be an effective strategy for the preparation of highly active sites and highly efficient water oxidation catalysts [51]. Inspired by these results, electropolymerization of molecular catalysts with specific functional groups on carbon materials has attracted increasing attentions for OER [51], oxygen reduction reaction (ORR) [52], and carbon dioxide reduction reaction (CO₂RR) [53].

* Corresponding authors.

E-mail addresses: leiht2017@snnu.edu.cn (H. Lei), ruicao@snnu.edu.cn (R. Cao).

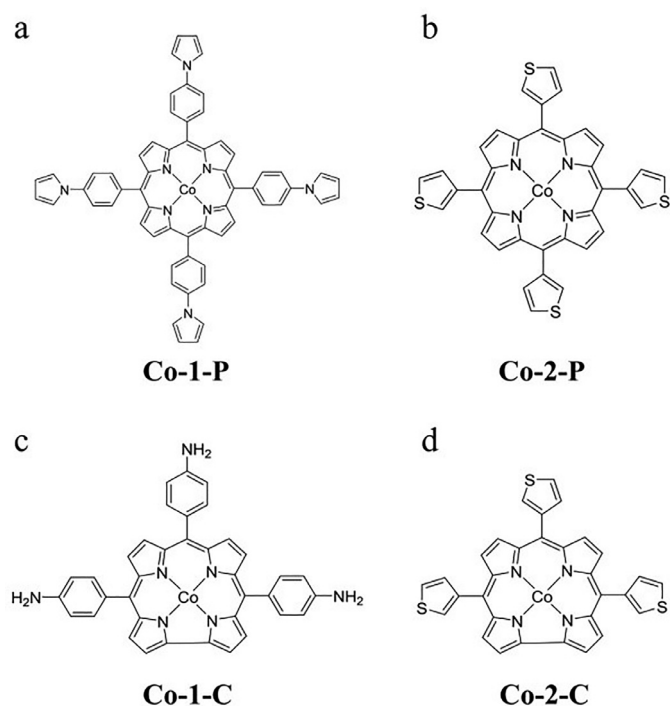


Fig. 1. Structure diagram of (a) **Co-1-P**, (b) **Co-2-P**, (c) **Co-1-C**, (d) **Co-2-C**.

Herein, we report the electropolymerization of Co porphyrins and corroles on conductive carbon cloth (CC) electrode for OER.

Four monomeric cobalt porphyrins and corroles with different functional groups were designed and used for polymerization. Metal-free porphyrins, tetrakis(*p*-*N*-pyrrolylphenyl)porphyrin (**1-P**) [54], tetrakis(thien-3-yl)-porphyrin (**2-P**) [55], 5,10,15-tris(4-aminophenyl)corrole (**1-C**) [52,56] and 5,10,15-tris(3-thienyl)corrole (**2-C**) [57,58] were synthesized by using literature methods, and their purity was verified by mass spectrometry (Figs. S3, S5, S8, S10 in Supporting information). The reaction of porphyrin and corrole ligands with Co salts afforded **Co-1-P**, **Co-2-P**, **Co-1-C** and **Co-2-C**, respectively (Fig. 1). The purity of the bulk samples of **Co-1-P**, **Co-2-P**, **Co-1-C** and **Co-2-C** was confirmed by mass spectrometry (Figs. S4, S6, S9, S11 in Supporting information). The cyclic voltammograms (CVs) of these Co complexes were recorded in dry acetonitrile solution containing 0.1 mol/L Bu_4NPF_6 . In general, **Co-1-P**, **Co-2-P** and **Co-1-C** showed two redox events, while **Co-2-C** showed three redox events (Figs. S12–S15 in Supporting information). This result also proved the purity of these four complexes.

Electropolymerization was conducted by using a CC electrode as the working electrode. The CC electrode was dipped into an acetonitrile solution containing 0.1 mol/L Bu_4NPF_6 and a specific Co complex (1 mmol/L) with the use of a carbon rod as the auxiliary electrode and Ag/AgNO_3 as the reference electrode [59,60]. After 60 cycles scanning between 0 V and 1.7 V (vs. ferrocene) under N_2 , the working electrode was gently rinsed with dichloromethane and ethanol, and then was finally dried at room temperature under dark.

After electropolymerization, the resulted hybrids were analyzed by X-ray photoelectron spectroscopy (XPS), scanning electron microscopy (SEM) and energy dispersive X-ray (EDX) element mapping, showing the absence of irregular particles of metal porphyrins and corroles (Fig. 2 and Fig. S16 in Supporting information). As shown in Fig. 2, comparing to bare CC electrodes (Fig. 2a), **Co-1-P@CC** exhibited significant complex loading (Fig. 2b). The SEM image of **Co-1-P@CC** (Fig. 2c) and the corresponding EDX elemental mapping images of C (Fig. 2d), N (Fig. 2e) and Co (Fig. 2f)

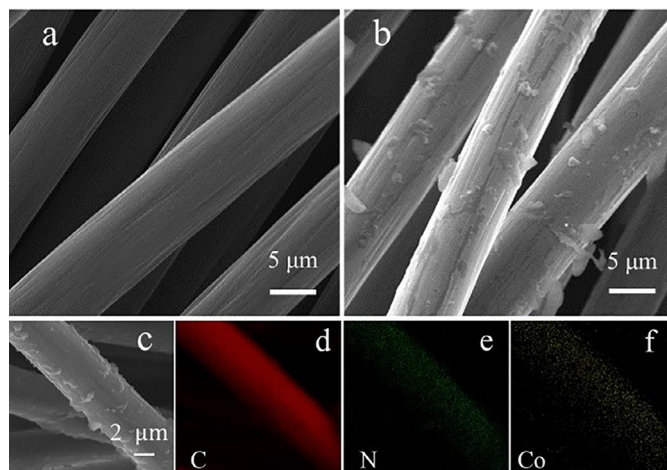


Fig. 2. (a) SEM images of blank CC. (b, c) SEM images of **Co-1-P@CC**. (d-f) Corresponding elemental mapping of **Co-1-P@CC**.

clearly confirmed the electrodeposition and uniform distribution of Co porphyrins on the surfaces of CC electrode. Moreover, the XPS analysis of **Co-1-P@CC** showed signals attributed to Co 2p (796.8 and 780.6 eV), which is identical to that of **Co-1-P** molecular complex, further confirming the presence of **Co-1-P** on CC electrode (Fig. S17 in Supporting information). For **Co-2-P**, **Co-1-P** and **Co-2-C**, XPS (Figs. S18–20 in Supporting information) and EDX elemental mapping (Figs. S21–23 in Supporting information) results clearly showed signals of Co, N and C, further confirming the presence of these Co porphyrins and corroles in their electrodeposited films. Moreover, **Co-1-P**, **Co-2-P**, **Co-1-C** and **Co-2-C** were analyzed by Raman. Comparing to the simply adsorbed monomeric Co porphyrin and Co corrole on CC electrodes, electropolymerized films displayed the decrease of the I_D/I_G ratio (Figs. S24–27 in Supporting information). This result indicates that polymerization reaction occurred between the molecules.

A three-electrode system was selected to test the OER property of electropolymerized samples in 0.1 mol/L KOH solutions. As shown in Fig. 3a, the blank CC exhibited very poor catalytic current of OER. The linear sweep voltammetry (LSV) of **Co-1-P@CC** displayed a significant catalytic current with the onset potential of 1.61 V versus RHE (reversible hydrogen electrode, all potentials recorded in aqueous solutions are referenced to RHE unless otherwise noted). This value corresponds to an onset overpotential of 380 mV, which is smaller than those of **Co-2-P@CC** (409 mV), **Co-1-C@CC** (430 mV) and **Co-2-C@CC** (405 mV). Particularly, **Co-1-P@CC** revealed the highest current density under the same applied potentials (i.e., 1.75 V). Encouraged by the above results, we also studied the effects of electroplating times on catalytic performance. As shown in Fig. 3b, the catalytic current increased with the increase of the electrodeposition CV cycle numbers. However, **Co-1-P** is easily fallen away from the CC electrode after more than 60-cycle CV. Thus, CC electrodes electropolymerized through 60-cycle CV were used for the following measurements. In addition, we normalized the activity with the amount of Co contents on CC electrode. The Co contents of four samples were determined by the inductively coupled plasma mass spectrometry (ICP-MS, Table S1 in Supporting information). As shown in Fig. 3c, **Co-1-P@CC** still displayed the highest catalytic performance. Tafel slope of **Co-1-P@CC** (70.8 mV/dec) is smaller than that of **Co-2-P@CC** (85.5 mV/dec), **Co-1-C@CC** (96.9 mV/dec) and **Co-2-C@CC** (156.3 mV/dec), indicating good kinetics during OER (Fig. 3d).

Controlled potential electrolysis (CPE) for OER in 0.1 mol/L KOH solutions was performed to examine the catalyst stability. The currents of **Co-1-P@CC** were constant in 10 h electrolysis (Fig. 4a). The

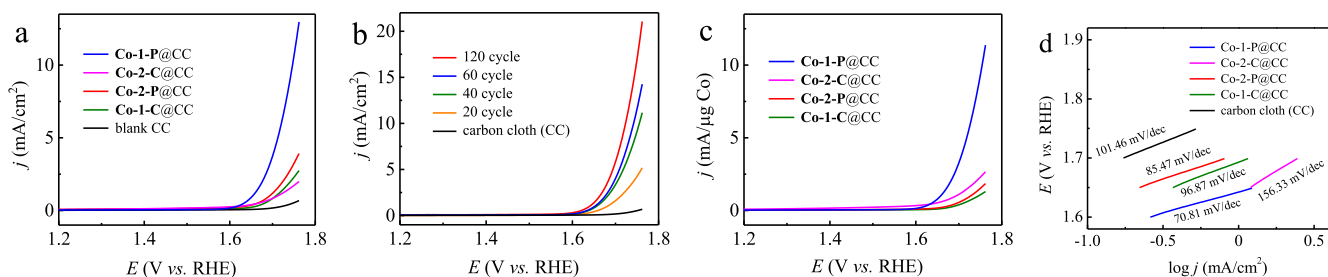


Fig. 3. (a) LSVs of blank CC, **Co-1-P@CC**, **Co-2-P@CC**, **Co-1-C@CC** and **Co-2-C@CC** in 0.1 mol/L KOH solution with a scan rate of 10 mV/s. (b) LSVs of **Co-1-P@CC** electrodes prepared from different CV cycle numbers. (c) Normalized OER activities by Co content. (d) Tafel slopes of blank CC, **Co-1-P@CC**, **Co-2-P@CC**, **Co-1-C@CC** and **Co-2-C@CC**.

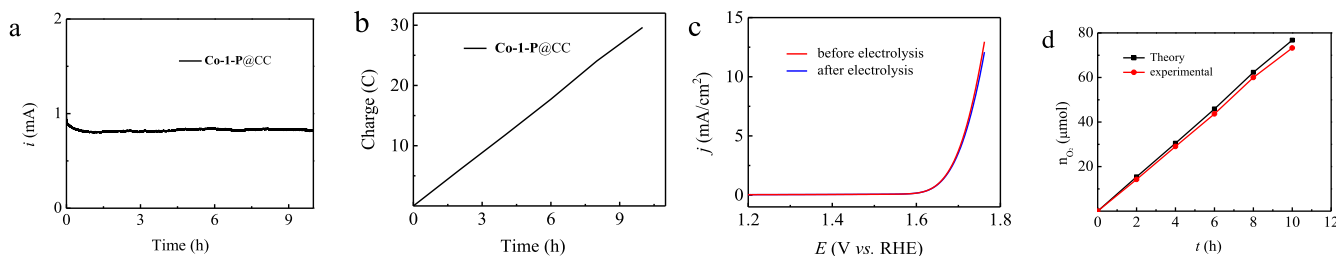


Fig. 4. (a) Controlled potential electrolysis of **Co-1-P@CC** at 1.65 V in 0.1 mol/L KOH solutions. (b) The electric charge curve of **Co-1-P@CC** during 10 h CPE. (c) LSV scans of **Co-1-P@CC** before and after electrolysis. (d) Gas chromatography detection of evolved O_2 during electrolysis with **Co-1-P@CC** at 1.65 V and the theoretical amount of O_2 produced.

corrected electric charges accumulated during electrolysis have a linear dependence on the time (Fig. 4b), which is a further line of evidence of the robustness of **Co-1-P@CC**. After CPE, the electrode was analyzed, showing almost identical LSV scans of **Co-1-P@CC** before and after electrolysis (Fig. 4c). These results are supportive of the catalyst stability for water oxidation. During electrolysis, O_2 gas bubbles were generated on the electrode surface. By using a gas-tight electrochemical cell, the amount of O_2 formed on the headspace can be determined by gas chromatography, which gave a Faradaic efficiency > 95% (Fig. 4d).

In summary, a simple electropolymerization method has been developed to immobilize molecules of Co porphyrins and corroles on conductive carbon substrates. The resulted catalyst, **Co-1-P@CC**, display an onset overpotential of 380 mV for OER and a Tafel slope of 70.8 mV/dec in 0.1 mol/L KOH solutions and show high stability over 10 h CPE. In addition, the electrocatalysts is tightly attached to the electrode substrate to form a monolithic electrode without using any binder polymer, increasing stability during the catalytic process and reducing overpotential due to ohmic resistance. This work provides a new strategy by loading active species onto a solid surface for water splitting reactions, which is valuable to be explored in other electrocatalytic processes.

Declaration of competing interest

There are no conflicts to declare.

Acknowledgements

We are grateful for support from National Natural Science Foundation of China (Nos. 21773146 and 21902099), China Postdoctoral Science Foundation (No. 2018M631120), Shaanxi Province Postdoctoral Science Foundation (No. 2018BSHEDZZ107), Fundamental Research Funds for the Central Universities (Nos. GK202103045 and GK202103050), Research funds of Shaanxi Normal University, and the open fund of State Key Laboratory of Structural Chemistry.

Supplementary materials

Supplementary material associated with this article can be found, in the online version, at doi:10.1016/j.ccllet.2021.04.048.

Reference

- W. Zhang, W. Lai, R. Cao, Chem. Rev. 117 (2017) 3717–3797.
- H. Lei, H. Fang, Y. Han, et al., ACS Catal. 5 (2015) 5145–5153.
- B. Wang, X. Cui, J. Huang, R. Cao, Q. Zhang, Chin. Chem. Lett. 29 (2018) 1757–1767.
- H. Lei, X. Li, J. Meng, et al., ACS Catal. 9 (2019) 4320–4344.
- X.-P. Zhang, A. Chandra, Y.-M. Lee, et al., Chem. Soc. Rev. (2021), doi:10.1039/d0cs01456g.
- Y. Liu, Y. Han, Z. Zhang, et al., Chem. Sci. 10 (2019) 2613–2622.
- R. Blankenship, D. Tiede, J. Barber, et al., Science 332 (2011) 805–809.
- D. Gust, T. Moore, A. Moore, Acc. Chem. Res. 42 (2009) 1890–1898.
- Y. Tong, H. Liu, M. Dai, L. Xiao, X. Wu, Chin. Chem. Lett. 31 (2020) 2295–2299.
- G. Xu, H. Lei, G. Zhou, et al., Chem. Commun. 55 (2019) 12647–12650.
- M.G. Walter, E.L. Warren, J.R. McKone, et al., Chem. Rev. 110 (2010) 6446–6473.
- X. Gao, Y. Chen, T. Sun, et al., Small 15 (2019) e1904579.
- H. Lei, A. Han, F. Li, et al., Phys. Chem. Chem. Phys. 16 (2014) 1883–1893.
- X. Guo, N. Wang, X. Li, et al., Angew. Chem. Int. Ed. 59 (2020) 8941–8946.
- H.J. Choi, N. Ashok Kumar, J.B. Baek, Nanoscale 7 (2015) 6991–6998.
- Z. Chen, D. Higgins, A. Yu, L. Zhang, J. Zhang, Energy Environ. Sci. 4 (2011) 3167–3192.
- Y. Nie, L. Li, Z. Wei, Chem. Soc. Rev. 44 (2015) 2168–2201.
- Y. Deng, L. Yang, Y. Wang, et al., Chin. Chem. Lett. 32 (2021) 511–515.
- C. Wang, L. Jin, H. Shang, et al., Chin. Chem. Lett. (2020), doi:10.1016/j.ccllet.2020.11.051.
- H. Qin, Y. Wang, B. Wang, et al., J. Energy Chem. 53 (2021) 77–81.
- T. Nakazono, A.R. Parent, K. Sakai, Chem. Commun. 49 (2013) 6325–6327.
- D. Wang, J.T. Groves, Proc. Natl. Acad. Sci. U.S.A. 110 (2013) 15579–15584.
- J.D. Blakemore, R.H. Crabtree, G.W. Brudvig, Chem. Rev. 115 (2015) 12974–13005.
- D.K. Dogutan, Jr. McGuire R., D.G. Nocera, J. Am. Chem. Soc. 133 (2011) 9178–9180.
- D.G. Hettler, J.N. Reek, Angew. Chem. Int. Ed. 51 (2012) 9740–9747.
- M.D. Kärkäs, O. Verho, E.V. Johnston, B. Åkerman, Chem. Rev. 114 (2014) 11863–12001.
- M.M. Najafpour, G. Renger, M. Holynska, et al., Chem. Rev. 116 (2016) 2886–2936.
- W. Schofberger, F. Faschinger, S. Chattopadhyay, et al., Angew. Chem. Int. Ed. 55 (2016) 2350–2355.
- W. Sinha, A. Mizrahi, A. Mahammed, B. Tumanski, Z. Gross, Inorg. Chem. 57 (2018) 478–485.
- B. Wurster, D. Grumelli, D. Hötger, R. Gutzler, K. Kern, J. Am. Chem. Soc. 138 (2016) 3623–3626.

- [31] L. Xu, H. Lei, Z. Zhang, et al., *Phys. Chem. Chem. Phys.* 19 (2017) 9755–9761.
- [32] Y. Han, Y. Wu, W. Lai, R. Cao, *Inorg. Chem.* 54 (2015) 5604–5613.
- [33] Z. Liang, H. Guo, G. Zhou, et al., *Angew. Chem. Int. Ed.* 60 (2021) 8472–8476.
- [34] L. Xie, X.-P. Zhang, B. Zhao, et al., *Angew. Chem. Int. Ed.* 60 (2021) 7576–7581.
- [35] Z. Liang, H. Wang, H. Zheng, W. Zhang, R. Cao, *Chem. Soc. Rev.* 50 (2021) 2540–2581.
- [36] L. Xie, X. Li, B. Wang, et al., *Angew. Chem. Int. Ed.* 58 (2019) 18883–18887.
- [37] L. Xie, J. Tian, Y. Ouyang, et al., *Angew. Chem. Int. Ed.* 59 (2020) 15844–15848.
- [38] X. Li, H. Lei, J. Liu, et al., *Angew. Chem. Int. Ed.* 57 (2018) 15070–15075.
- [39] Z. Chen, J.J. Concepcion, H. Luo, et al., *J. Am. Chem. Soc.* 132 (2010) 17670–17673.
- [40] E.L. Demeter, S.L. Hilburg, N.R. Washburn, T.J. Collins, J.R. Kitchin, *J. Am. Chem. Soc.* 136 (2014) 5603–5606.
- [41] S. Gentil, D. Serre, C. Philouze, et al., *Angew. Chem. Int. Ed.* 55 (2016) 2517–2520.
- [42] I. Hijazi, T. Bourgeteau, R. Cornut, et al., *J. Am. Chem. Soc.* 136 (2014) 6348–6354.
- [43] M. Jahan, Q. Bao, K.P. Loh, *J. Am. Chem. Soc.* 134 (2012) 6707–6713.
- [44] P. Kang, S. Zhang, T.J. Meyer, M. Brookhart, *Angew. Chem. Int. Ed.* 53 (2014) 8709–8713.
- [45] A. Maurin, M. Robert, *J. Am. Chem. Soc.* 138 (2016) 2492–2495.
- [46] S. Kim, D. Jang, J. Lim, et al., *Chem. Sus. Chem.* 10 (2017) 3473–3481.
- [47] M. Tavakkoli, M. Nosek, J. Sainio, et al., *ACS Catal.* 7 (2017) 8033–8041.
- [48] P.D. Tran, A. Le Goff, J. Heidkamp, et al., *Angew. Chem. Int. Ed.* 50 (2011) 1371–1374.
- [49] P.J. Wei, G.Q. Yu, Y. Naruta, J.G. Liu, *Angew. Chem. Int. Ed.* 53 (2014) 6659–6663.
- [50] J. Wang, L. Xu, T. Wang, et al., *Adv. Energy Mater.* (2021) 2003575.
- [51] D.L. Ashford, A.M. Lapidus, A.K. Vannucci, et al., *J. Am. Chem. Soc.* 136 (2014) 6578–6581.
- [52] A. Friedman, L. Landau, S. Gonen, Z. Gross, L. Elbaz, *ACS Catal.* 8 (2018) 5024–5031.
- [53] X.M. Hu, Z. Salmi, M. Lillethorup, et al., *Chem. Commun.* 52 (2016) 5864–5867.
- [54] A. Bettelheim, B.A. White, S.A. Raybuck, R.W. Murray, *Inorg. Chem.* 26 (1987) 1009–1017.
- [55] W. Chen, J. Akhigbe, C.B. Ckner, C.M. Li, Y. Lei, *J. Phys. Chem. C* 114 (2010) 8633–8638.
- [56] M.G. Walter, C.C. Wamser, *J. Phys. Chem. C* 114 (2010) 7563–7574.
- [57] N. Maiti, J. Lee, S.J. Kwon, et al., *Polyhedron* 25 (2006) 1519–1530.
- [58] N. Maiti, J. Lee, Y. Do, H.S. Shin, D.G. Churchill, *J. Chem. Crystallogr.* 35 (2005) 949–955.
- [59] A.N. Marianov, Y. Jiang, *ACS Sustainable Chem. Eng.* 7 (2019) 3838–3848.
- [60] A.N. Marianov, Y. Jiang, *Appl. Catal. B* 244 (2019) 881–888.